nature

SUPPLEMENTARY INFORMATION

https://doi.org/10.1038/s41586-018-0174-3

In the format provided by the authors and unedited.

Phase-separation mechanism for C-terminal hyperphosphorylation of RNA polymerase II

Huasong Lu[1,2], Dan Yu[2], Anders S. Hansen[2], Sourav Ganguly[2], Rongdiao Liu[1], Alec Heckert[2], Xavier Darzacq[2] & Qiang Zhou[2]*

[1]School of Pharmaceutical Sciences, Xiamen University, Xiamen, China. [2]Department of Molecular and Cell Biology, University of California, Berkeley, CA, USA. *e-mail: qzhou@berkeley.edu

Supplementary Figure 1: Uncropped scans with size marker indications

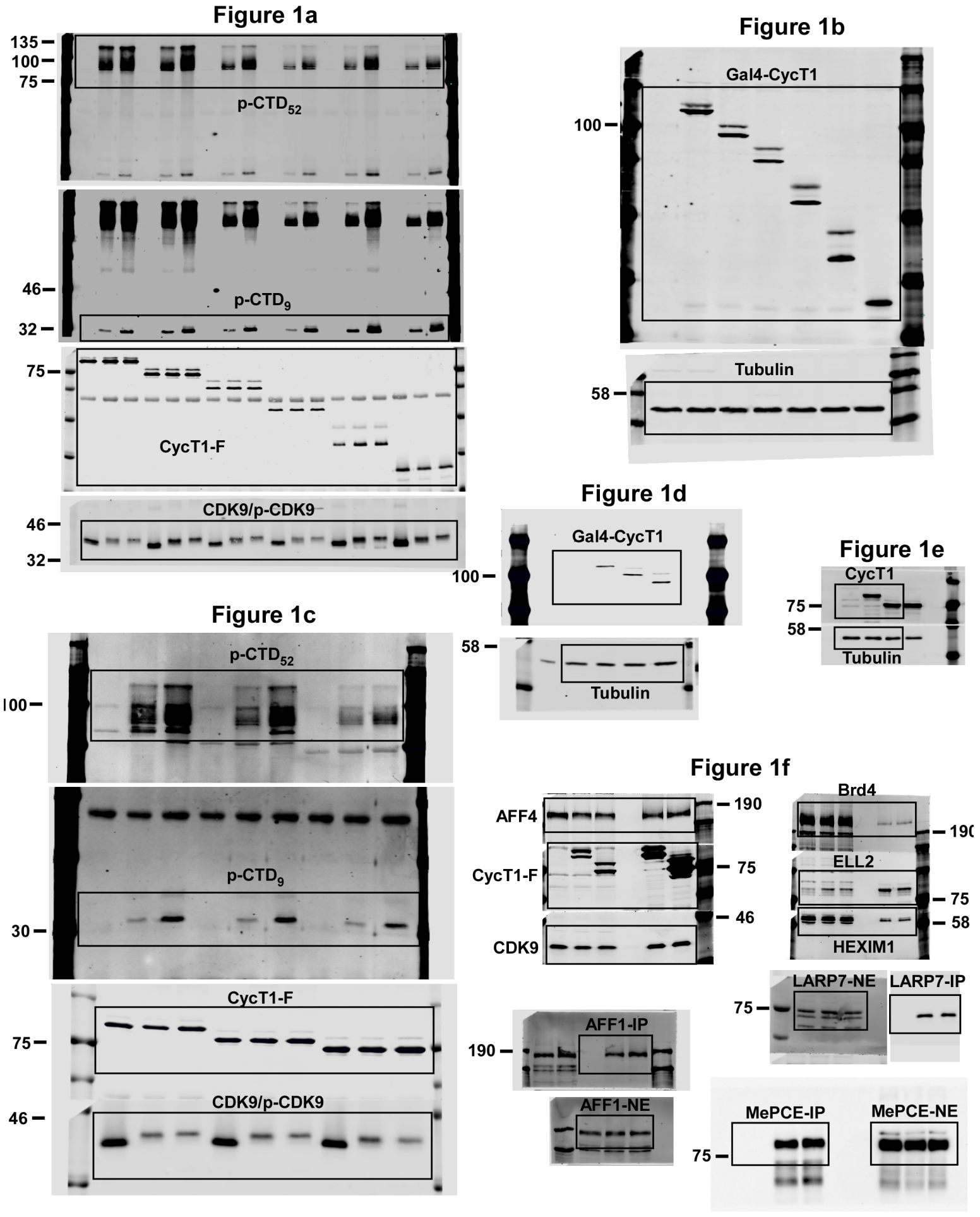

Figure 2a

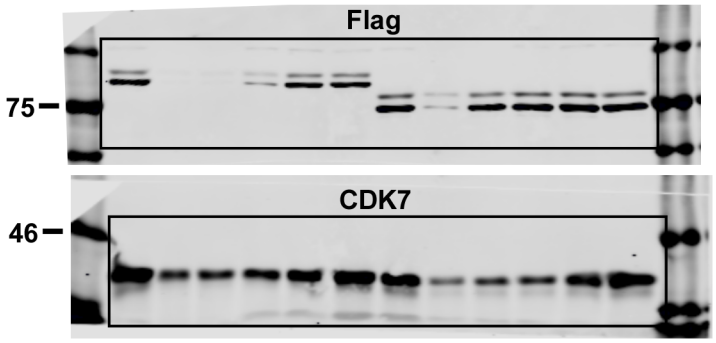

Figure 2f

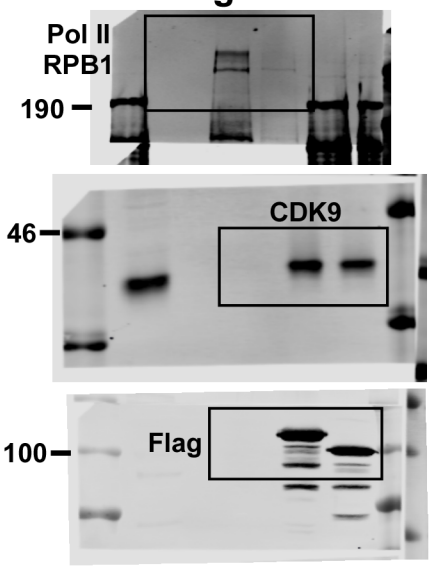

Figure 2g

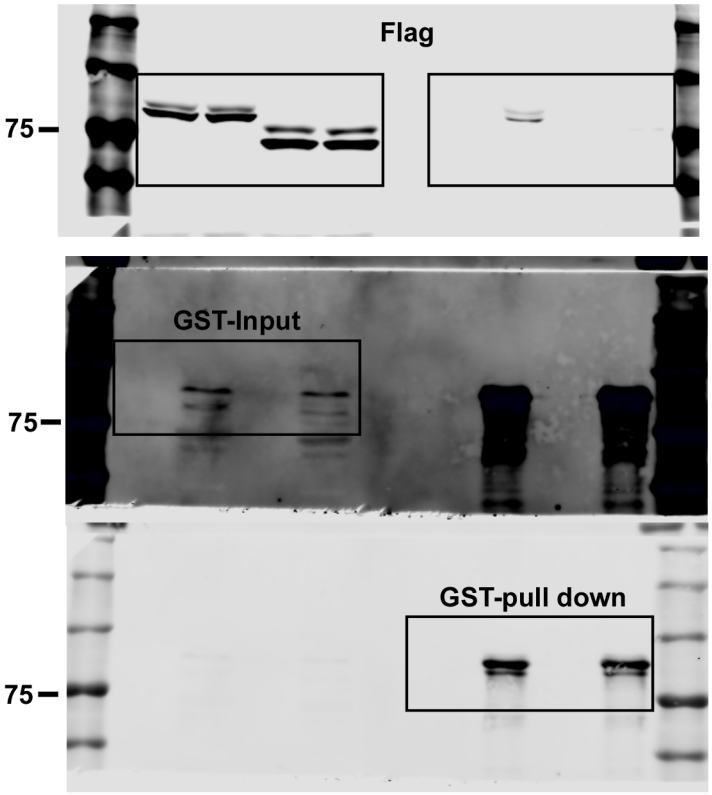

Figure 3a

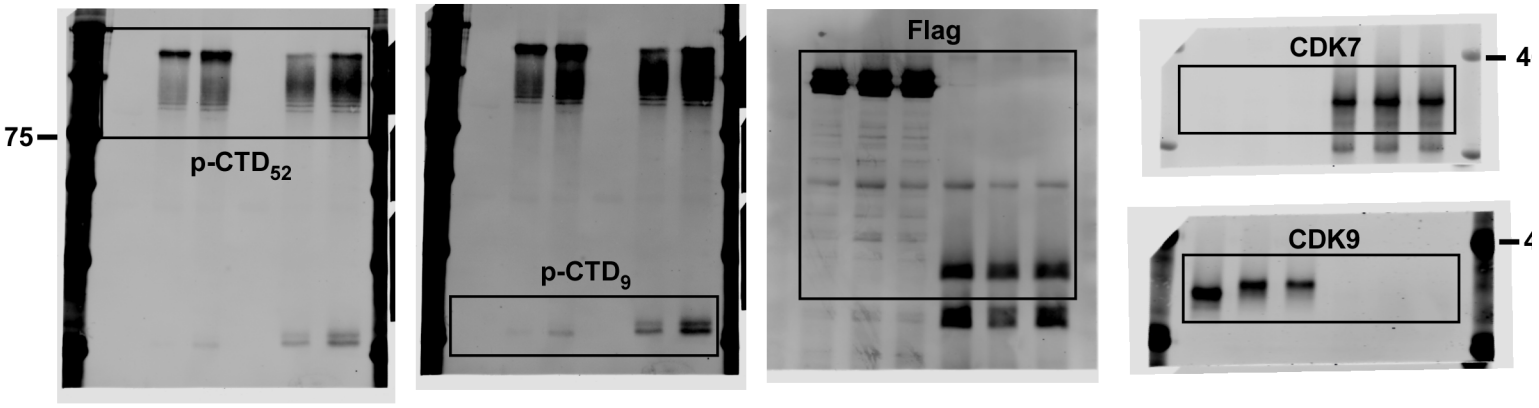

Figure 3b

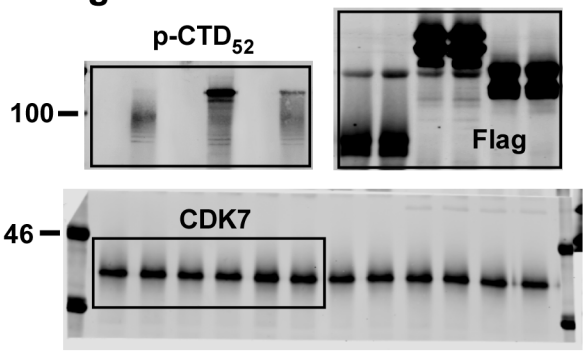

Figure 3c

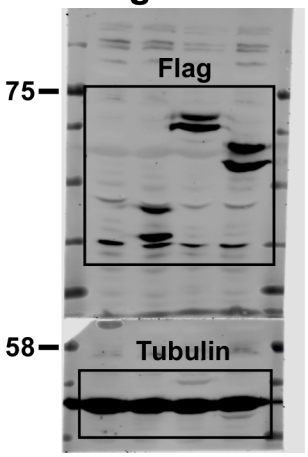

Figure 3d

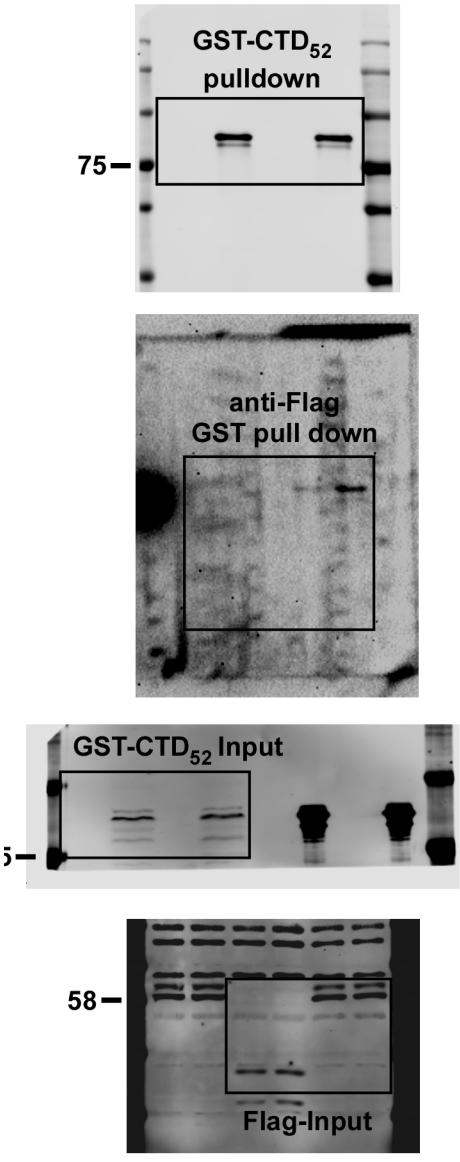

Figure 3e

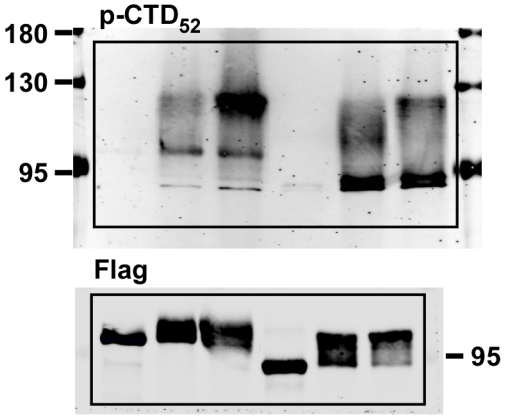

Figure 3f

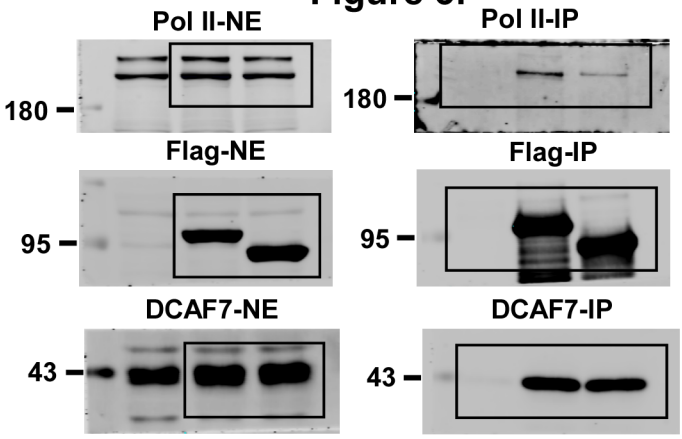

Figure 4g

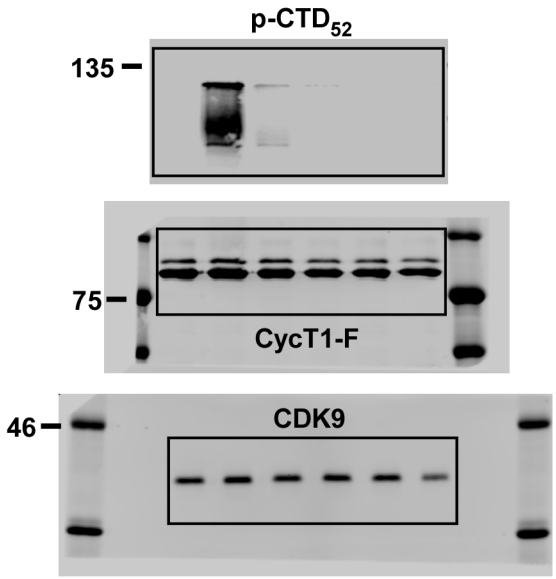

Figure 4i

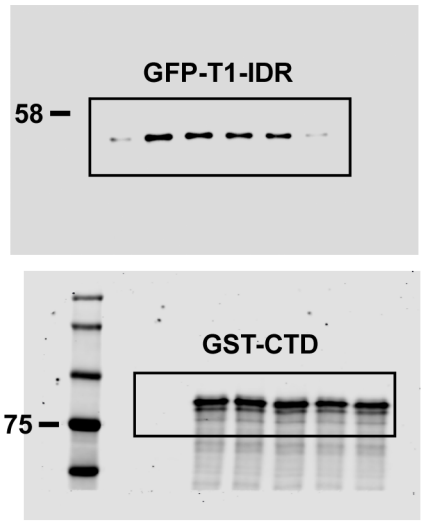

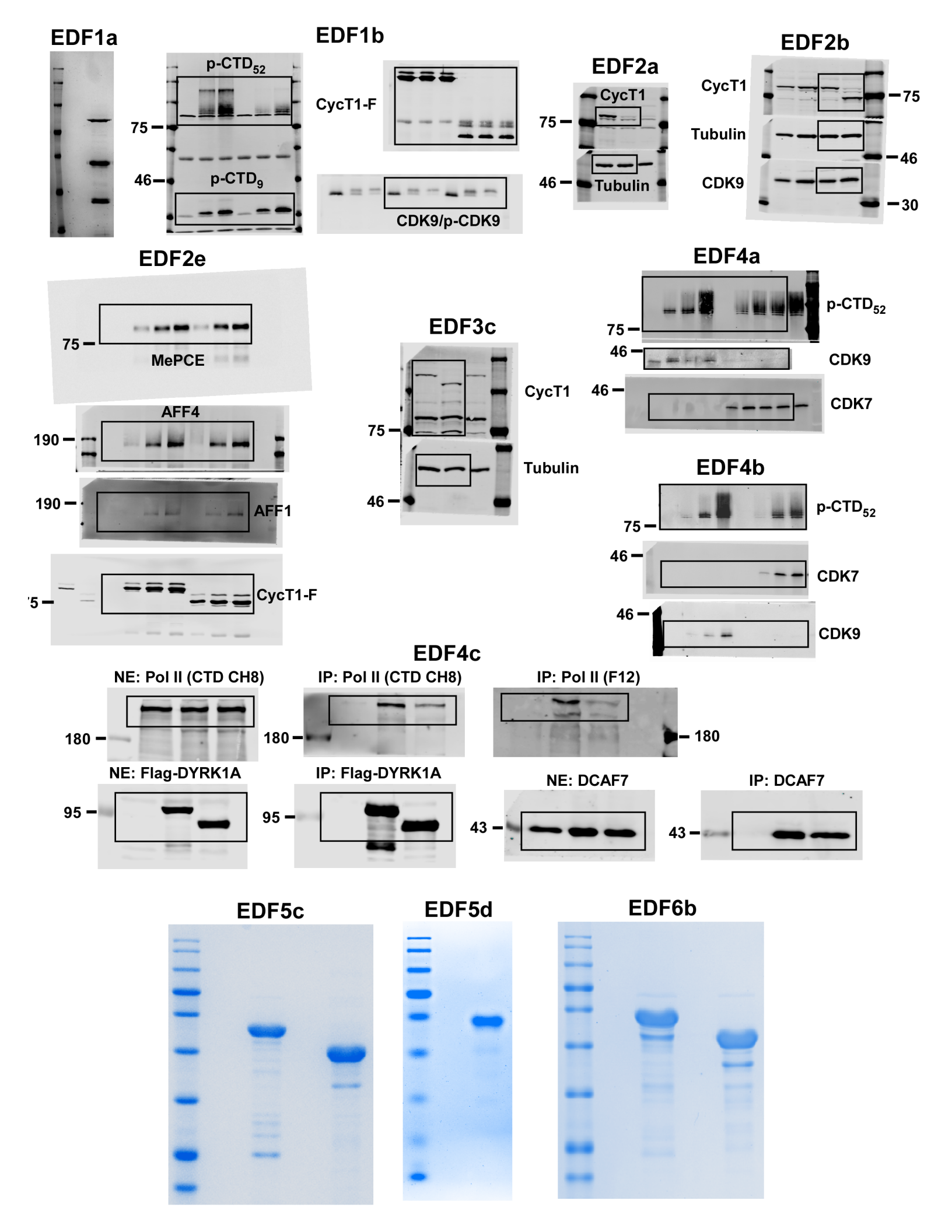
EDF1a
EDF1b
p-CTD52
75
46
p-CTD9
CycT1-F
CDK9/p-CDK9
EDF2a
CycT1
75
46
Tubulin
EDF2b
CycT1
Tubulin
CDK9
75
46
30
EDF2e
75
MePCE
AFF4
190
AFF1
190
CycT1-F
EDF3c
CycT1
75
Tubulin
46
EDF4a
p-CTD52
75
46
CDK9
46
CDK7
EDF4b
p-CTD52
75
46
CDK7
46
CDK9
EDF4c
NE: Pol II (CTD CH8)
IP: Pol II (CTD CH8)
IP: Pol II (F12)
180
180
180
NE: Flag-DYRK1A
IP: Flag-DYRK1A
95
95
NE: DCAF7
IP: DCAF7
43
43
EDF5c
EDF5d
EDF6b

EDF7b

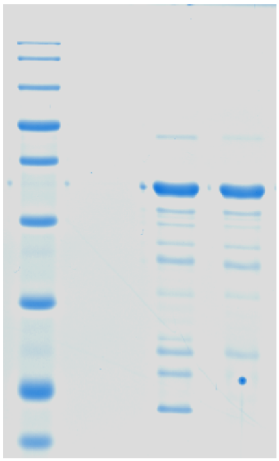

EDF7c

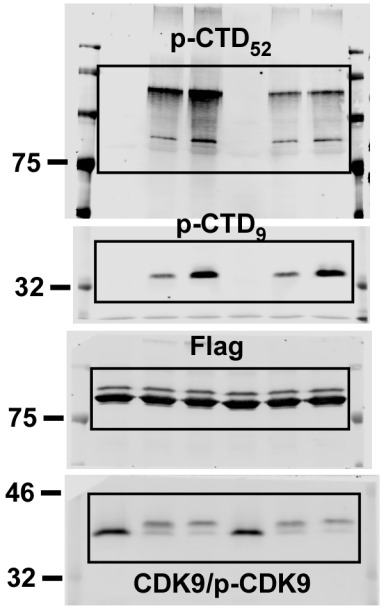

EDF7d

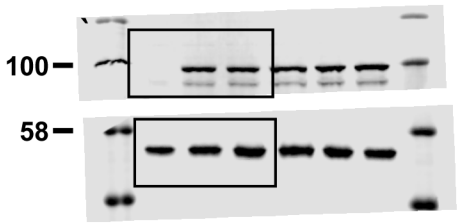

EDF8a

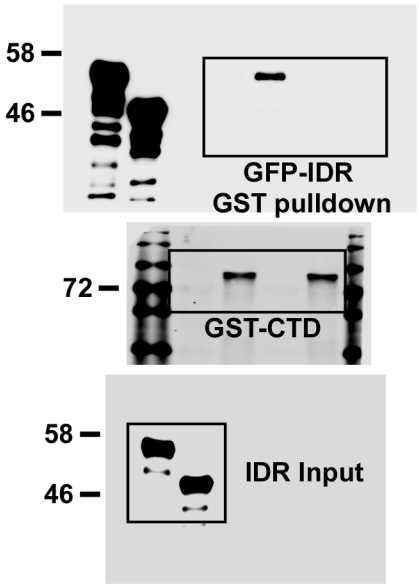

EDF8c

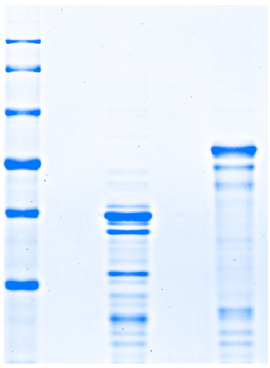

EDF8d

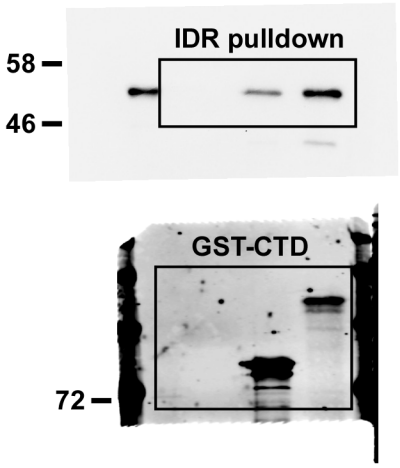

EDF8b

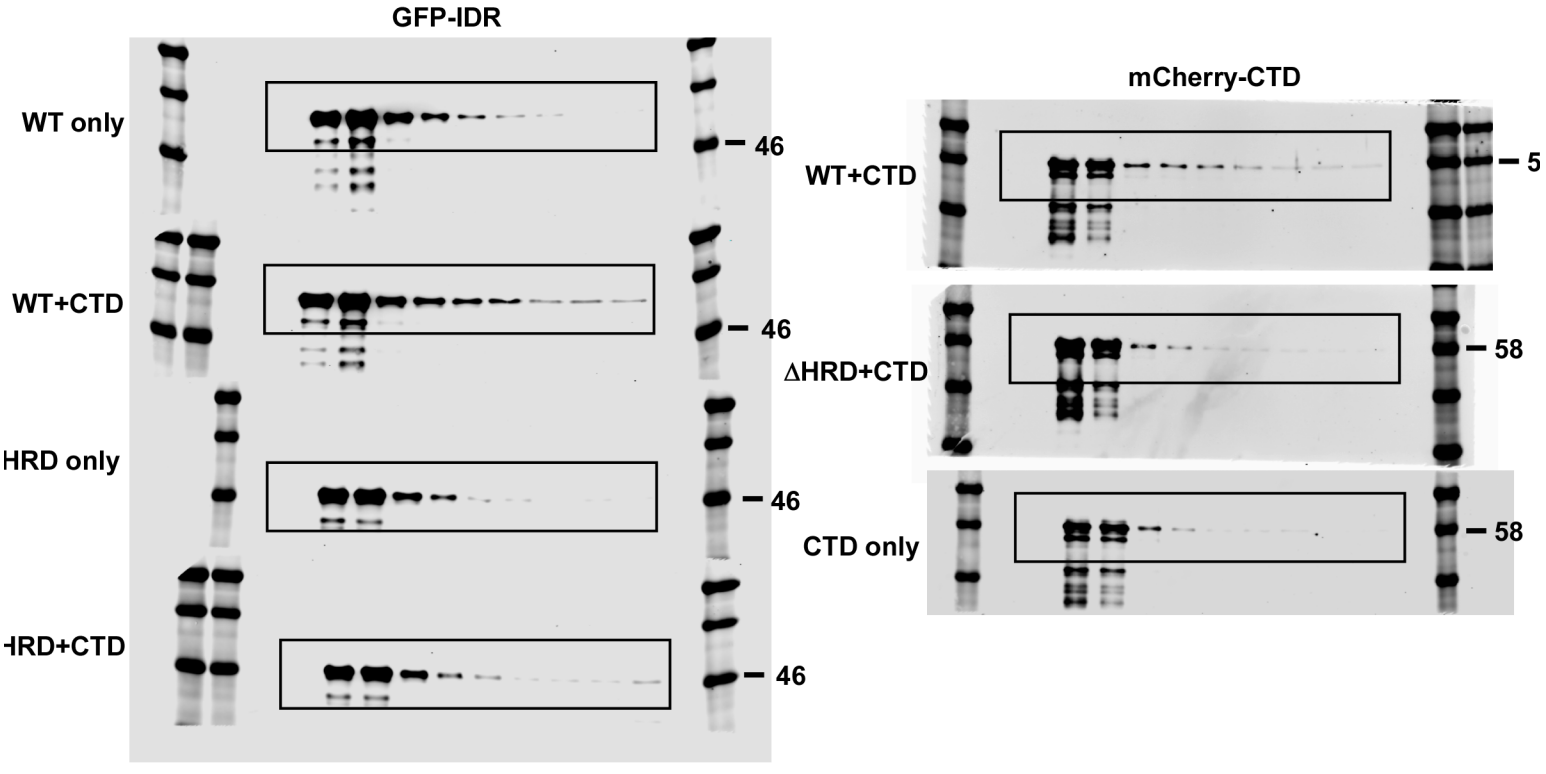

Methods

Antibodies, plasmids and cell lines

The following antibodies were purchased from commercial sources: AFF1 (Bethyl Laboratories, Cat. #A302-344A), AFF4 (Abcam, Cat. # ab57077), ELL2 (Bethyl Laboratories, Cat. # A302-505A), MePCE (Bethyl Laboratories, Cat. # A304-184A), RNA Pol II phospho-Ser2 (Millipore, Cat. # 04-1571), RNA Pol II phospho-Ser5 (Millipore, Cat. # 04-1572), and CDK7 (Sigma, Cat. # C7089-.2ML). The RPB1 subunit of RNA Pol II in Fig. 2f and Fig. 3f was detected with sc-56767 and sc-899X (Santa Cruz Biotech), respectively. Antibodies against CDK9, LARP7, HEXIM1 and Brd4 were generated in our own laboratory and have been described previously[1,2].

The 6xUAS-LTR-luciferase reporter construct contained the HIV-1 LTR promoter sequence with six repeats of the Gal4 upstream activation sequence (UAS) inserted upstream of the Sp1-binding sites. All Gal4 fusion proteins contained the DNA-binding domain (DBD) of Gal4 (aa1–147) attached to the N-termini of the various CycT1, CycH and CycH+T1 proteins and were expressed from the pcDNA3 expression vector (Thermo Fisher Scientific). The halo-tag was fused to the N-terminus of CycT1 or CycT1ΔHRD in pcDNA3. The lentiviral vector pLKO.1 (Addgene) expressing the CycT1-specific shRNA (shCycT1) has been described previously to generate the stable HeLa-based CycT1 KD clone[3]. The DNA fragments encoding WT CycT1-IDR, WT DYRK1A-IDR and their ΔHRD derivatives were amplified by PCR and inserted into the pGFP-2xStrep expression vector (kindly provided by the Hurley lab, UC Berkeley). The sequences of all plasmids were confirmed by DNA sequencing. The plasmids expressing mCherry-CTD (containing CTD repeats 27-52) and GST-CTD_9 were kindly provided by

the McKnight lab (UTSW)[4] and Geyer lab (University of Bonn, Germany)[5], respectively. All cell lines (HeLa, HEK293T and U2OS) were authenticated at UC Berkeley Cell Culture Facility by single nucleotide polymorphism testing and confirmed as mycoplasma negative.

In vitro kinase assay

The kinase complex containing the indicated CycT1-F, CycH-F, CycH+T1-F, F-DYRK1A, or their derivatives was affinity-purified using the anti-Flag agarose beads (Sigma) under high salt plus detergent (1M KCl + 1% NP-40) conditions. The purified proteins still attached to the Flag beads were incubated with 100 ng recombinant GST-CTD_{52} and 100 ng GST-CTD_9 at 30 °C in a 25 μl reaction that also contained 50 mM HEPES pH 7.3, 50 mM NaCl, 1 mM DTT, 10 mM $MgCl_2$, and 0.1 mM ATP. The reactions testing DYRK1A also contained 10 mM $MnCl_2$. For reactions containing recombinant kinase complexes, CDK7-CycH-MAT1 (CAK) and CDK9-CycT1 (P-TEFb) were purchased from Millipore. The kinase reactions were stopped at different time points by the addition of 10 μl of the SDS-PAGE sample-loading buffer. After heating at 95 °C for 10 min, the samples were analyzed by SDS-PAGE and Western blotting with the indicated antibodies.

GST pull-down assay

GST-CTD_{52} (2 μg) were incubated with HeLa nuclear extracts (400 μl) containing the indicated Flag-tagged proteins for 3 hr at 4°C, and purified by using the glutathione-Sepharose beads (GE Healthcare) according to the manufacturer's protocol. For interaction between GST-CycT1 and endogenous RNA Pol II, HeLa nuclear extracts (400 μl) were incubated with GST or the different GST-CycT1 fusion proteins (5 μg)

immobilized on glutathione-Sepharose beads for 3 hr at 4 °C. After the incubation, the beads were washed extensively with buffer D [20 mM HEPES-KOH (pH 7.9), 15% (vol/vol) glycerol, 0.2 mM EDTA, 0.2% NP-40, 1 mM DTT, 1 mM PMSF, and 0.3 M KCl] and then directly boiled in 20 μl SDS-PAGE sample-loading buffer. The materials were analyzed by Western blotting with the indicated antibodies.

Differential salt extractions

HeLa cells ($2x10^7$) transfected with the indicated expression constructs were suspended in buffer A (10 mM Tris·HCl pH 7.5, 10 mM NaCl, 3 mM $MgCl_2$, 0.5% NP-40, and 2.5 mM DTT), incubated on ice for 10 min, and then centrifuged at 4,000 rpm for 10 min. Nuclear pellets were resuspended in 500 μl buffer A, and aliquots (100 μl) were then incubated in the presence of increasing concentrations of NaCl from 10 to 200 mM. After centrifugation for 10 min at 14,000 rpm, 15 μl of the supernatants were analyzed by SDS-PAGE and Western blotting.

FRAP assay and data analysis

U2OS cells containing the integrated genomic array[6] were plated at a density of $1x10^4$ cells per well in LabTek chambered coverslips (Nunc, Denmark) and transfected with either LacI-YFP/Tet-ON/halo-CycT1 or LacI-YFP/Tet-ON/halo-CycT1ΔHRD plasmids (0.5 μg of each plasmid). At 24-36 hr post-transfection, cells were labeled with halo-TMR ligand (1 μM, Promega) prior to imaging. Doxycycline (1 μg/ml) was added to the media post transfection and maintained during imaging. Fluorescence images were acquired at room temperature on inverted Zeiss LSM 710 confocal microscope (Jena, Germany) with a 63x, 1.4 NA oil immersion objective lens. The 561 nm line of a DPSS laser was used for excitation of halo-TMR, while the 514 nm line of the argon laser was

used to image the LacI-YFP in a separate channel. Emission for halo-TMR was collected between 565-630 nm, while for YFP emission was collected between 520-550 nm.

Photobleaching of halo-TMR was accomplished using maximal power of the 561 nm laser line. FRAP experiments were carried out under the same conditions as mentioned above. Imaging conditions were pre-established such that the intensity of the laser used to monitor fluorescence of halo-TMR did not induce significant bleaching. The fluorescence of LacI-YFP was used to mark the genomic array as a region of interest (ROI; ~1.2 μm), and FRAP of the protein of interest was performed in the corresponding ROI in the halo-TMR channel.

For nonlinear curve fitting and quantitative analysis, data representing the mean fluorescence intensity of the monitored ROI were background subtracted using a ROI placed outside the cell, and corrected for moderate cellular movement and photobleaching during scanning. Fluorescence recovery plots with fluorescence intensities normalized to pre-bleach intensities were analyzed based on a reaction-diffusion (RD) model that simultaneously accounts for binding interactions and diffusion as described previously[7-9]. When the association time of a protein with its binding site is comparable with the time it would take for the protein to diffuse freely through the bleach spot, diffusion and binding can no longer be simplified to unique analytical expressions. Under these conditions, binding interactions are intricately coupled to the diffusion of the proteins, and therefore both binding and diffusion aspects need to be simultaneously analyzed.

The RD model has analytical expression as a Laplace transform solution shown below:

$$I_L(p) = \left(\frac{1 - C_{eq}}{p}\right)\left(1 + \frac{k_{on}^*}{p + k_{off}}\right)(2K_1(qw)I_1(qw))$$

where I_L is the fluorescence intensity in Laplacian space, p is the Laplacian variable (inverse of time), w is the bleach spot dimension, k^*_{on} is the pseudo-on rate, k_{off} is the off-rate, $C_{eq} = \frac{k^*_{on}}{k^*_{on}+k_{off}}$ is the bound fraction, $q^2 = \left(\frac{p}{D_{app}}\right)\left(1+\frac{k^*_{on}}{p+k_{off}}\right)$ and D_{app} is the apparent diffusion coefficient. The Laplace transform is inverted numerically. The actual FRAP data was logarithmically binned and fitted to the following equation,

$$I(t) = 1 - \varphi + \varphi\left(L^{-1}(I_L(p))\right)$$

where $I(t)$ is the logarithmically binned FRAP data, φ is the fraction photobleached, and L^{-1} is for inverse Laplacian.

Three independent variables, namely k^*_{on}, k_{off}, and D_{app} were extracted from the fitting. The parameter space of k^*_{on} and k_{off} were first globally sampled to generate initial values avoiding local minima. These initial values were subsequently used to optimize all three parameters together. The fourth parameter, C_{eq} (or the bound fraction) is derived using the recovered values for k^*_{on} and k_{off}, using the relationship $C_{eq} = k^*_{on}/(k^*_{on} + k_{off})$. The errors mentioned for the recovered parameters are as derived from the fit. Analysis of images, including correction for cellular movement and photobleaching, and non-linear regression of fluorescence recovery data were performed using custom written scripts in Matlab version 2016b (Mathworks, MA, USA).

Single-particle tracking (spaSPT and slowSPT)

U2OS cells stably expressing halo-tagged WT or ΔHRD CycT1 to about 70% of the endogenous CycT1 level or H2B-halo-SNAP[10] were grown overnight on plasma-cleaned 25 mm circular no 1.5H cover glasses (Marienfeld High-Precision 0117650). After overnight growth, cells were labeled with 50 nM PA-JF_{549}[11] for spaSPT

experiments or with 10 pM JF646[12] for slowSPT for ~30 min and washed twice (one wash: medium removed; PBS wash; replenished with fresh medium). At the end of the final wash, cells were placed in phenol red-free medium.

Single-particle tracking was performed on a custom-built Nikon TI microscope equipped with a 100x/NA 1.49 oil-immersion TIRF objective (Nikon apochromat CFI Apo TIRF 100x Oil), EM-CCD camera (Andor iXon Ultra 897; frame-transfer mode; vertical shift speed: 0.9 μs; -70°C), a perfect focusing system to correct for axial drift and motorized laser illumination (Ti-TIRF, Nikon), which allows an incident angle adjustment to achieve highly inclined and laminated optical sheet illumination[13]. An incubation chamber maintained a humidified 37°C atmosphere with 5% CO_2 and the objective was also heated to 37°C. Excitation was achieved using a 561 nm (1 W, Genesis Coherent) laser for PA-JF_{549} and 633 nm (1 W, Genesis Coherent) for JF_{646} and photo-activation achieved using a 405 nm laser (140 mW, OBIS, Coherent). The excitation laser was modulated by an acousto-optic tunable filter (AA Opto-Electronic, AOTFnC-VIS-TN) and triggered with the camera TTL exposure output signal. The laser light was coupled into the microscope by an optical fiber and then reflected using a multi-band dichroic (405 nm/488 nm/561 nm/633 nm quad-band, Semrock) and then focused in the back focal plane of the objective. Fluorescence emission light was filtered using a single band-pass filter placed in front of the camera using the following filters (PA-JF549: Semrock 593/40 nm bandpass filter). The microscope, cameras, and hardware were controlled through NIS-Elements software (Nikon).

We performed two types of single-particle tracking: a “fast” mode for following both bound and fast-diffusing molecules and a “slow” mode for focusing specifically on

bound molecules. In the "fast" mode, we recorded single-particle tracking movies using our previously developed technique, stroboscopic photo-activation Single-Particle Tracking (spaSPT)[10,14]. Briefly, 1 ms 561 nm excitation (100% AOTF) of PA-JF_{549} was delivered at the beginning of the frame to minimize motion-blurring; 405 nm photo-activation pulses were delivered during the camera integration time (~447 μs) to minimize background and their intensity optimized to achieve a mean density of ~1 molecule per frame per nucleus. 30,000 frames were recorded per cell per experiment. The camera exposure time was 10 ms resulting in a frame rate of approximately 95 Hz (7 ms + ~447 μs per frame).

For single-particle tracking in the "slow" mode, we used constant 633 nm excitation and long exposure times (500 ms) to deliberately motion-blur out fast-diffusing molecules and thus preferentially detect bound molecules as previously described[15]. We then recorded movies of 2,400 frames corresponding to 20 min.

spaSPT data was analyzed (localization and tracking) and converted into trajectories using a custom-written Matlab implementation of the MTT-algorithm[16] and the following settings: Localization error: $10^{-6.25}$; deflation loops: 0; Blinking (frames): 1; max competitors: 3; max D ($\mu m^2/s$): 20.

slowSPT data was analyzed (localization and tracking) and converted into trajectories using a custom-written Matlab implementation of the MTT-algorithm[16] and the following settings: Localization error: $10^{-6.25}$; deflation loops: 0; Blinking (frames): 2; max competitors: 5; max D ($\mu m^2/s$): 0.08.

Analysis of single-particle spaSPT data using Spot-On

To analyze the spaSPT data, we used our previously described kinetic modeling approach (Spot-On)[10,14]. Briefly, each replicate was analyzed separately and the subpopulation fractions and free diffusion constants were reported as the mean +/- standard deviation from each replicate. We merged the data from all cells (~5-10) for each replicate, compiled histograms of displacements and then fit the displacement cumulative distribution functions for 6 time points using a 3-state model that assumes that halo-CycT1 can either exist in a chromatin-bound or one of two freely diffusive states: a slow and a fast state:

$$P_3(r,\Delta\tau) = F_{\mathrm{BOUND}}\frac{r}{2(D_{\mathrm{BOUND}}\Delta\tau+\sigma^2)}e^{\frac{-r^2}{4(D_{\mathrm{BOUND}}\Delta\tau+\sigma^2)}} + Z_{\mathrm{CORR}}(\Delta\tau,\Delta z_{\mathrm{corr}},D_{\mathrm{SLOW}})F_{\mathrm{SLOW}}\frac{r}{2(D_{\mathrm{SLOW}}\Delta\tau+\sigma^2)}e^{\frac{-r^2}{4(D_{\mathrm{SLOW}}\Delta\tau+\sigma^2)}} + Z_{\mathrm{CORR}}(\Delta\tau,\Delta z_{\mathrm{corr}},D_{\mathrm{FAST}})(1-F_{\mathrm{BOUND}} - F_{\mathrm{SLOW}})\frac{r}{2(D_{\mathrm{FAST}}\Delta\tau+\sigma^2)}e^{\frac{-r^2}{4(D_{\mathrm{FAST}}\Delta\tau+\sigma^2)}}$$

where:

$$Z_{\mathrm{CORR}}(\Delta\tau) = \frac{1}{\Delta z}\int_{-\Delta z/2}^{\Delta z/2}\left\{1 - \sum_{n=0}^{\infty}(-1)^n\left[\mathrm{erfc}\left(\frac{\frac{(2n+1)\Delta z}{2}-z}{\sqrt{4D_{\mathrm{FREE}}\Delta\tau}}\right)+\mathrm{erfc}\left(\frac{\frac{(2n+1)\Delta z}{2}+z}{\sqrt{4D_{\mathrm{FREE}}\Delta\tau}}\right)\right]\right\}\mathrm{d}z$$

and:

$$\Delta z = 0.700\ \mu\mathrm{m} + 0.24179\mathrm{s}^{-1/2}\sqrt{D} + 0.20521\ \mu\mathrm{m}$$

Here, F_{BOUND} is the fraction of molecules that are bound to chromatin, D_{BOUND} is the diffusion constant of chromatin bound molecules, D_{SLOW} is diffusion constant of the slow subpopulation of freely diffusing molecules, D_{FAST} is the diffusion constant of the slow subpopulation of freely diffusing molecules, r is the displacement length, $\Delta\tau$ is lag time between frames, Δz is axial detection range, σ is localization error and Z_{CORR} corrects for defocalization bias (i.e. the fact that freely diffusion molecules gradually move out-of-focus, but chromatin bound molecules do not). In this case, the use of a 3-state model instead of a 2-state model was motivated by the fact that a 2-state model was insufficiently able to fit the data in accordance with Izeddin *et al* [17].

Model fitting and parameter optimization was performed using a non-linear least squares algorithm (Levenberg-Marquardt) implemented in the Matlab version of Spot-On (v1.0; GitLab tag 92cdf210) and the following parameters: dZ=0.7 μm; GapsAllowed=1; TimePoints: 6; JumpsToConsider=4; ModelFit=2; NumberOfStates=3; FitLocError=0; LocError=0.04; D_Free1_3State=[0.5;25]; D_Free1_3State=[0.5;25]; D_Bound_3State=[0.00001;0.04].

Analysis of "slow" single-particle tracking data

To analyze the data, we calculated the survival probability distribution (1-CDF), i.e. the fraction of molecules still bound as a function of time. Often this distribution is fit with either a single- or double-exponential function to extract residence times. However, we found that the halo-CycT1 distribution was not well-fit with such functions, most likely because the protein is unlike traditional transcription factors and does not unbind with a single rate-limiting step. For this reason, we did not fit the survival probability distribution and hence no residence times were reported. Nevertheless, from inspection of

the survival probability distribution, it is very clear that WT halo-CycT1 displayed more stable binding than did the ΔHRD mutant.

Phase-separated droplet formation

All GFP- and mCherry-fusion proteins were expressed in 1 liter of *E. coli* BL21 cells upon induction overnight with 0.25 mM IPTG at 16 ºC. Harvested cells were resuspended in 30 ml lysis buffer (50 mM Tris-HCl pH7.5, 500 mM NaCl, 1 mM DTT, 1% Triton X-100) and lysed by sonication (40% output, 16 cycles of 15 sec on and 60 sec off). After centrifugation at 11,500 rpm for 1 hr, the soluble fractions of the lysates were loaded onto the Ni-NTA resin (Thermo) for the His-tagged protein or the Strep-Tactin column (IBA GmbH) for the Strep-tagged proteins according to the protocols provided by the manufacturers. After extensive washes with the washing buffer (20 mM Tris-HCl pH7.5, 500 mM NaCl, 1 mM DTT, 1% NP-40, and 0.1 mM PMSF), the bound proteins were eluted with 3ml of the same buffer containing 200 mM imidazole (for His-tag) or 10 mM desthiobiotin (for Strep-tag). The proteins were then dialyzed overnight at 4℃ against 150 mM NaCl, 20 mM Tris pH7.5, and 1 mM DTT. After the dialysis, the purified proteins were concentrated with Amicon ultra centrifugal filters (Millipore) and stored at -80 ºC. The purity of the proteins was examined by SDS-PAGE and Coomassie Blue staining and their concentrations determined by the Bradford assay in combination with Coomassie Blue staining.

The droplet formation assay was performed as described previously[18]. To facilitate the formation of phase-separated liquid droplets, the various fusion proteins were diluted to a final concentration as indicated in the relevant figure legends in a buffer containing 20 mM Tris-HCl pH 7.5, 1 mM DTT and 37.5 mM NaCl. 5 μl of the protein solution was trapped between two coverslips and images were acquired on either an epifluorescence microscope (EVOS FL, Thermo) or a confocal microscope (Zeiss

LSM710).

To examine the impact of CAK-catalyzed mCherry-CTD pre-phosphorylation on latter's incorporation into the GFP-T1-IDR phase-separated droplets, 120 μg mCherry-CTD was incubated with affinity-purified CDK7-CycH-F-Mat1 immobilized on 15 μl Flag beads or just empty Flag beads as a negative control in a 30 μl kinase reaction (50 mM HEPES pH 7.3, 50 mM NaCl, 1 mM DTT, 10 mM $MgCl_2$, and 1 mM ATP) for 6 hours at 30 °C to ensure saturated phosphorylation. To initiate phase-separation, the collected supernatants from the kinase reactions containing phosphorylated or unphosphorylated mCherry-CTD (at 1.2 mg/ml final concentration) were mixed with GFP-T1-IDR at 3 mg/ml in a solution that also contained 52.5 mM NaCl. Images were acquired on a Zeiss LSM710 confocal microscope.

Immunofluorescence and time-lapse phase contrast imaging of cells

HeLa cells were plated on glass coverslips in 6-well plates and transfected with the indicated expression constructs. At 40 hr post-transfection, the cells were fixed in 4% paraformaldehyde for 10 min at RT. The coverslips were rinsed twice with PBS and the cells were permeabilized with 0.2% Triton X-100 in PBS for 10 min and blocked with 5% normal donkey serum for 1 hr. The cells were stained with relevant primary antibodies (1:1000 for anti-Flag, 1:200 for anti-CycT1) for 1 hour at RT, followed by incubation with the corresponding secondary antibodies conjugated to Alexa Fluor 488 (1:400) for 45 min at room temperature in the dark. After washing in PBS for four times, the coverslips were mounted on glass slides using Vectashield (Vector Laboratories) and imaged on a Zeiss LSM710 confocal microscope.

Time-lapse phase contrast imaging was described previously[19]. Briefly, live HeLa

cells expressing eGFP-CycT1 at a level similar to that of endogenous CycT1 were examined on MatTek coverslips with a Nikon BioStation IMq time-lapse microscope at 50% intensity. During image acquisition, cells were incubated in an equilibrated observation chamber at 37˚ C and with 5% CO_2. Images were acquired at 5-minute intervals across the coverslip. The images were loaded and compared in ImageJ to identify fusion events.

Data availability

Uncropped scans for all western blots are provided in Supplementary Figure 1. The raw slowSPT and spaSPT data are freely available in Spot-On readable CSV and Matlab formats in the form of single-molecule trajectories at Zenodo: https://zenodo.org/record/1215836. The Spot-On Matlab code is available together with a step-by-step guide at Gitlab: https://gitlab.com/tjian-darzacq-lab/spot-on-matlab. All other data are available from the corresponding author on reasonable request.

References for Methods

1 He, N. *et al.* A La-related protein modulates 7SK snRNP integrity to suppress P-TEFb-dependent transcriptional elongation and tumorigenesis. *Molecular cell* **29**, 588-599, doi:10.1016/j.molcel.2008.01.003 (2008).

2 Yang, Z. *et al.* Recruitment of P-TEFb for stimulation of transcriptional elongation by the bromodomain protein Brd4. *Molecular cell* **19**, 535-545, doi:10.1016/j.molcel.2005.06.029 (2005).

3 Lu, H. *et al.* AFF1 is a ubiquitous P-TEFb partner to enable Tat extraction of P-TEFb from 7SK snRNP and formation of SECs for HIV transactivation. *Proceedings of the National Academy of Sciences of the United States of America* **111**, E15-24, doi:10.1073/pnas.1318503111 (2014).

4 Kato, M. *et al.* Cell-free formation of RNA granules: low complexity sequence domains form dynamic fibers within hydrogels. *Cell* **149**, 753-767, doi:10.1016/j.cell.2012.04.017 (2012).

5 Czudnochowski, N., Bosken, C. A. & Geyer, M. Serine-7 but not serine-5 phosphorylation primes RNA polymerase II CTD for P-TEFb recognition. *Nature communications* **3**, 842, doi:10.1038/ncomms1846 (2012).
6 Darzacq, X. *et al.* In vivo dynamics of RNA polymerase II transcription. *Nature structural & molecular biology* **14**, 796-806, doi:10.1038/nsmb1280 (2007).
7 McNally, J. G. Quantitative FRAP in analysis of molecular binding dynamics in vivo. *Methods in cell biology* **85**, 329-351, doi:10.1016/S0091-679X(08)85014-5 (2008).
8 Mueller, F., Wach, P. & McNally, J. G. Evidence for a common mode of transcription factor interaction with chromatin as revealed by improved quantitative fluorescence recovery after photobleaching. *Biophysical journal* **94**, 3323-3339, doi:10.1529/biophysj.107.123182 (2008).
9 Sprague, B. L., Pego, R. L., Stavreva, D. A. & McNally, J. G. Analysis of binding reactions by fluorescence recovery after photobleaching. *Biophysical journal* **86**, 3473-3495, doi:10.1529/biophysj.103.026765 (2004).
10 Hansen, A. S., Pustova, I., Cattoglio, C., Tjian, R. & Darzacq, X. CTCF and cohesin regulate chromatin loop stability with distinct dynamics. *eLife* **6**, doi:10.7554/eLife.25776 (2017).
11 Grimm, J. B. *et al.* Bright photoactivatable fluorophores for single-molecule imaging. *Nature methods* **13**, 985-988, doi:10.1038/nmeth.4034 (2016).
12 Grimm, J. B. *et al.* A general method to improve fluorophores for live-cell and single-molecule microscopy. *Nature methods* **12**, 244-250, 243 p following 250, doi:10.1038/nmeth.3256 (2015).
13 Tokunaga, M., Imamoto, N. & Sakata-Sogawa, K. Highly inclined thin illumination enables clear single-molecule imaging in cells. *Nature methods* **5**, 159-161, doi:10.1038/nmeth1171 (2008).
14 Hansen, A. S. *et al.* Robust model-based analysis of single-particle tracking experiments with Spot-On. *eLife* **7**, doi:10.7554/eLife.33125 (2018).
15 Watanabe, N. & Mitchison, T. J. Single-molecule speckle analysis of actin filament turnover in lamellipodia. *Science* **295**, 1083-1086, doi:10.1126/science.1067470 (2002).
16 Serge, A., Bertaux, N., Rigneault, H. & Marguet, D. Dynamic multiple-target tracing to probe spatiotemporal cartography of cell membranes. *Nature methods* **5**, 687-694, doi:10.1038/nmeth.1233 (2008).
17 Izeddin, I. *et al.* Single-molecule tracking in live cells reveals distinct target-search strategies of transcription factors in the nucleus. *eLife* **3**, doi:10.7554/eLife.02230 (2014).
18 Lin, Y., Protter, D. S., Rosen, M. K. & Parker, R. Formation and Maturation of Phase-Separated Liquid Droplets by RNA-Binding Proteins. *Molecular cell* **60**, 208-219, doi:10.1016/j.molcel.2015.08.018 (2015).
19 Teves, S. S. *et al.* A dynamic mode of mitotic bookmarking by transcription factors. *eLife* **5**, doi:10.7554/eLife.22280 (2016).